Gravity Wave Horizontal and Vertical Wavelengths: An Update of Measurements in the Mesopause Region (~80–100 km)

A. H. MANSON

Institute of Space and Atmospheric Studies, University of Saskatchewan, Saskatoon, Saskatchewan, Canada

(Manuscript received 20 March 1990, in final form 8 June 1990)

ABSTRACT

During 1985–86 a summary and review of gravity wave measurements was made by Reid. In particular a collation of 408 horizontal wavelengths was prepared, which included values from optical and radar methods. Since that time substantial new datasets have emerged from the Medium Frequency radars at Adelaide and Saskatoon, and from the CEDAR lidar at Urbana. These data are combined with the earlier collation to form composite figures. Questions are raised about the selectivity of the sounding systems.

1. Introduction

Gravity wave (GW) characteristics such as wavelengths and periods (observed and intrinsic) are a highly desirable commodity for an improved understanding of atmospheric processes, energetics, and momentum budget (e.g., Fritts 1984; Fritts and Rastogi 1985). The summary and review of gravity wave observations by Reid (1986) was of considerable value as it discussed all available data on mean flow accelerations, horizontal scales and phase velocities, and seasonal variations in gravity wave activity. In particular, Reid showed horizontal wavelengths plotted against the directly observed periods obtained from optical systems (noctilucent cloud photographs, emissions from OH (~85 km) and OI (558 nm, 97 km) layers) and radars (early results from the Medium Frequency (MF) systems at Adelaide and Saskatoon, and from the M.S.T. (VHF) systems at Poker Flat and Urbana). These data are used as a background in figures discussed later (1, 2, and 4) with the author's permission. There are 408 waves or observations shown, 41% from optical, and 59% from radar techniques, including 58 from the then new triple bistatic GRAVNET MF radar system at Saskatoon, (Meek et al. 1985), and a sampling from the single multibeam MF radar at Adelaide operating in a Doppler mode (Reid 1984; Vincent and Reid 1983).

Since that time further analysis of the raw data from Saskatoon and Adelaide has led to substantial additions to their early GW datasets; in fact each now provides more waves than in the earlier collation (Manson and Meek 1988; Reid and Vincent 1987). These are discussed and shown in section 2. A discussion of some of these new data has been given elsewhere by Reid (1989). Finally, Gardner and Voelz (1987) have shown a substantial set of gravity wave data from the CEDAR lidar at Urbana. Sounding of the sodium layer provides vertical wavelengths λ_z at observed periods, and use of the gravity wave dispersion relation provides estimates of the horizontal wavelengths λ_h. Both of these wavelengths are discussed and compared with other observations in section 3. Discussions of the possible selectivity or biases present in each observation system are included in the respective sections.

2. New gravity wave data from Saskatoon and Adelaide

a. Saskatoon

The GRAVNET system is thoroughly discussed in the references given above. However, briefly, it comprises three receiving systems at the corners of an approximately equilateral triangle of side ~40 km: at each site the horizontal wind for heights from ~65 to 110 km is measured by the spaced antenna (SA) method. For particular heights, "Winds from the atmospheric triangle of ~20 km side are then analyzed by cross-spectral analysis techniques to determine directly the period T, horizontal wavelength λ_h, phase velocity $c(\phi)$, and wave amplitude u'; and the actual background wind $\bar{u}$ allows, uniquely among gravity wave measurements, the intrinsic parameters (as seen by an observer moving with the wind) to be calculated (T^*, $c - \bar{u}$). The gravity wave dispersion relation then provides (intrinsic) vertical wavelengths λ_z," (Manson and Meek 1988). The asymptotic approximation (Hines 1974; Manson and Meek 1988) was adequate for the majority of calculations. For waves with periods longer than 500 minutes, the more general expression for wave ellipticity was used (Gossard and Hooke

Corresponding author address: A. H. Manson, Institute of Space Atmospheric Study, University of Saskatchewan, Saskatoon, Saskatchewan, CANADA S7N OWO.

1975), and for λ_z greater than ~30 km the full dispersion relation (Hines 1974, p. 276) was also necessary. The retention of the asymptotic approximation in these latter cases would lead to an underestimation of the vertical wavelength by typically 25%. Values for the various parameters in these equations were taken from Gossard and Hooke (1975, p. 19). The appropriately calculated $\lambda_z$are also then to be directly compared with observed λ_z, but the word "intrinsic" was used to emphasize that the dispersion relation was correctly used with intrinsic periods.

The total new set of 593 observations or waves are superimposed upon the earlier collection by Reid (1986) in Fig. 1: 50 days from all seasons of 1983–85 are included, and (real) heights involved range from ~70 to ~105 km. The "screened" region of the figure encompasses all the waves: they were rather evenly distributed with no stray values. Only small variations in season and height were noted by Manson and Meek (1988), so the showing of all new waves is legitimate.

A few comments on the overall figures are desirable. First, as noted earlier the original collation involves observed periods, as the intrinsic periods were, and are, generally not available. (Even the early GRAVNET data are plotted versus observed periods.) However, because of the large assemblage over all seasons, many measurements were likely carried out under low background wind conditions, hence the range of λ_h at any period is probably representative of that appropriate to the actual (intrinsic) periods. Secondly, we have added lines that are approximate limits for waves undergoing damping due to eddy viscosity; these follow Meek et al. (1985), Manson and Meek (1988) and Hines (1974, p. 279) in particular, and are calculated using the intrinsic periods. Values of 30–300 $m^2 s^{-1}$ are typical of the height region (Hocking 1985), so that waves to the right and between these lines would be subject to strong damping. The few waves in the collation between these lines (~6%) are consistent with this. Finally, regarding the new GRAVNET data, minimum λ_h values of 40 km are set by the triangle size, and maxima by the phase differences in the cross-spectral analysis and significance criteria. Limits on observed period T were 10–60 minutes, but Doppler shifting expands the distribution of T^* beyond that, although only 6% lie within and beyond the limiting damping lines. In this latter category, errors in T^* become large as $c - \bar{u}$ tends to zero, hence, the uncertainty arrows in this region. It is preferable to say that these waves have T^* of at least 200 minutes and are approaching critical levels. Although the GRAVNET method of analysis does not depend upon vertical coherence for the waves, "inspection of waves at a particular period show that many estimates separated by 3–6 km agree very well, probably representing multiple sampling of the same wave," (Manson and Meek 1988). Thus, waves from the new GRAVNET dataset were not all limited (by some unknown process) to just one height, but had some vertical extent.

In conclusion there is excellent agreement between this new dataset and the original collation, providing validity to both because of their independence. The observed limits for smaller periods at each λ_h, on the left side of the figure, are similar for the two datasets, and match the "79 km reflection limit" shown in Hines (1974); see also Meek et al. (1985). Also, the absence of long λ_h for longer periods (>60 minutes) is due to the GRAVNET limits on sampling triangle and data lengths rather than an absence of waves. It therefore seems quite inappropriate to provide a line of best fit to the data, due to system limits, and the clear indication of a broad distribution of λ_h for each period.

b. Adelaide

The Adelaide MF radar, operating in the Doppler mode with multiple narrow beams, is a quite unique system, which is well described in the references already given. A brief description is required however, to put the data into proper context. Radial velocities are measured in off-vertical Doppler radar beams, cross-spectral analysis applied and then the gravity wave polarization and dispersion relations used to measure/calculate the horizontal wavelengths and phase velocities as a function of periods (Reid and Vincent 1987). In this technique it has not proven possible, at least at this stage, to solve for the intrinsic period T^*, so data shown here will be for observed period T. The authors note that much of their data were obtained under conditions of weak background wind, so that their values of λ_h and T, "should provide a good measure of the scale of motions present . . . even without correcting for the Doppler shift in wave frequency," (Reid and Vincent 1987). Indeed 50% of the λ_h data incorporated into the figure discussed below are for these days, and the other 50% are not dramatically different in their position in the λ_h, T plots.

The complete new set of 414 total waves are superimposed upon the same earlier collation by Reid in Fig. 2: 21 days from all seasons of 1981–82 are included, and heights range from 80–100 km. Minimum system λ_h values are ~15 km, and maxima are set by significance criteria. Limits on observed periods are ~10–120 minutes depending on record length. It is important to note that some of the waves were selected by Reid and Vincent on the basis of their vertical coherence, also, (Reid, personal communication) they did not differ in their placement upon the λ_h, T plots (their Fig. 5) from waves appropriate to single heights. Two screened regions are shown in Fig. 2, as there are fewer (4%) in the long λ_h, T region. It is important to note that these λ_h are zonal or meridional components of the actual wavelengths. Hence, the full λ_h for a wave field isotropic in azimuth will be smaller by $\sqrt{2}$—this factor has *not* been applied to Fig. 2 because the ad-

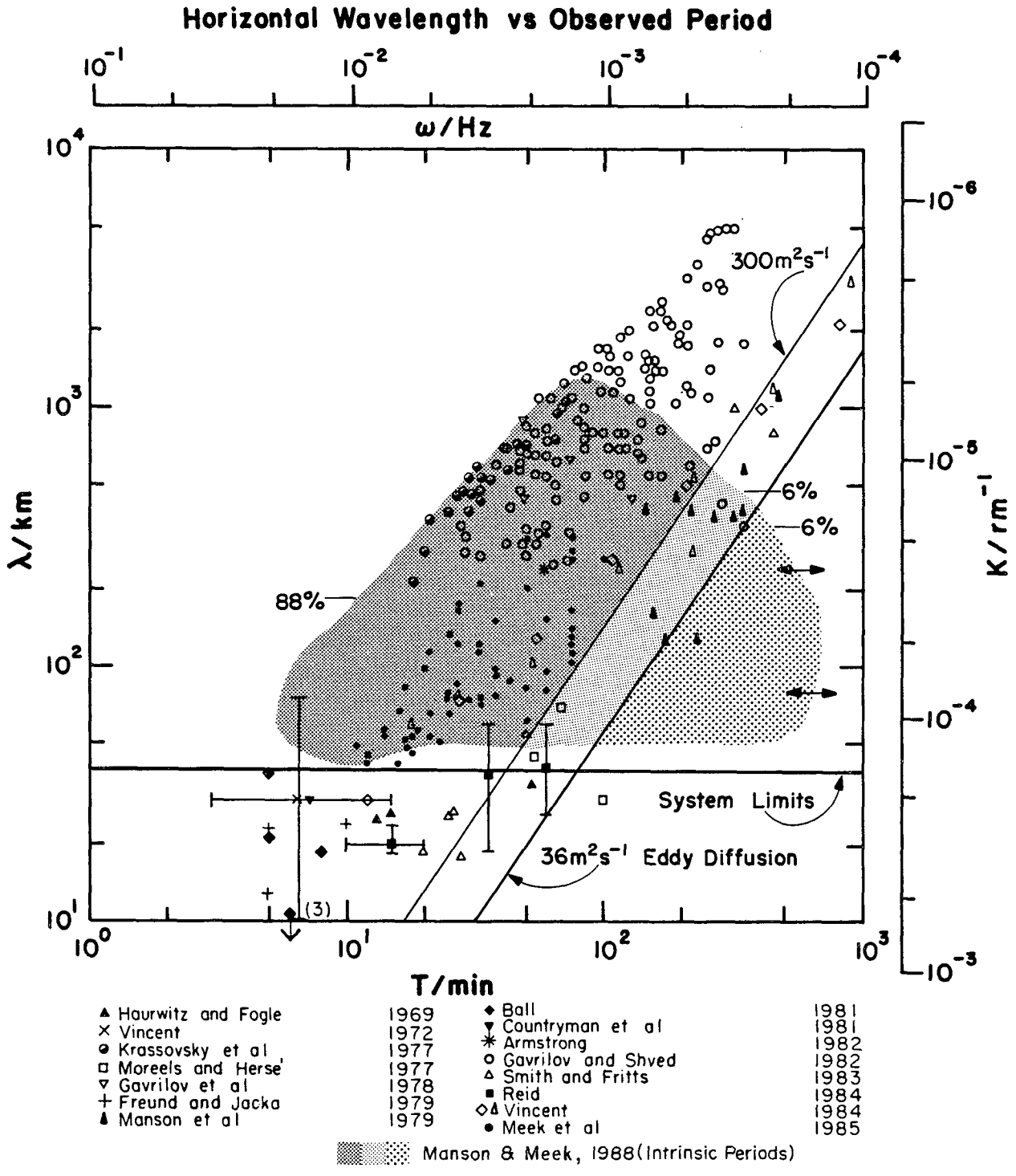

FIG. 1. "Collation of measurements of horizontal scale according to observed period for the 60–110 km height region for various locations and observing techniques. Vertical and horizonal bars indicate the range of values. A total of 408 observations are represented, with 59% from radar and 41% from optical (mainly 558 nm airglow) techniques. Most results (~75%) come from the 90–110 km height range." (Reid 1986). The Saskatoon GRAVNET data are shown by "toning" in the figure (Manson and Meek 1988). Measurements of background wind provide the *intrinsic* periods for these horizontal wavelengths: 50 days, 1983–85, 593 waves 70–105 km. Also, lines that are approximate limits for waves undergoing damping due to eddy viscosity are added; percentages in the regions about the lines are given. (System limits: observed periods 10–60 minutes, λ_{min} = 40 km).

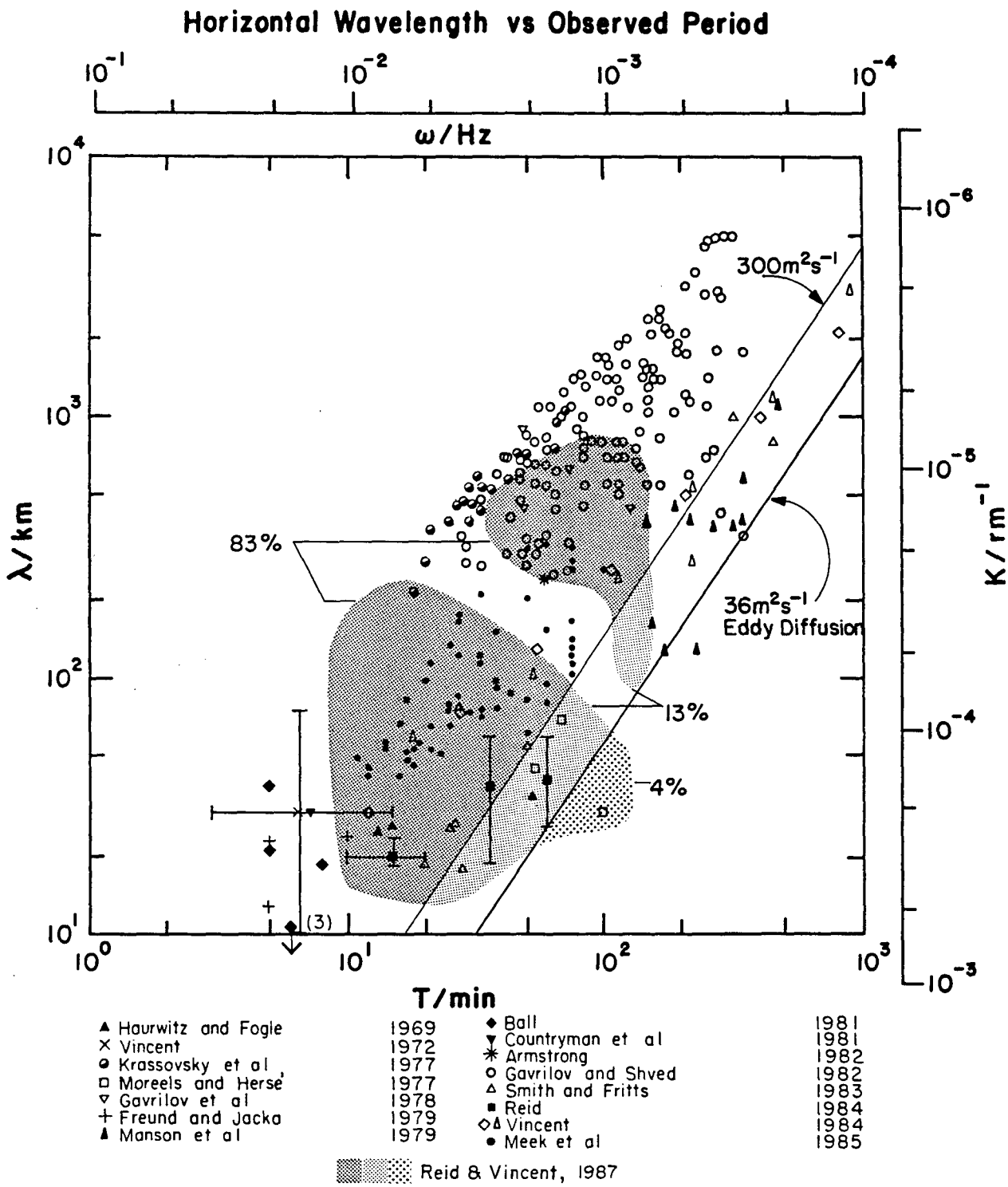

FIG. 2. As in Fig. 1, but the additional data are now from Reid and Vincent (1987). These are from the large "single multibeam" Adelaide MF radar, using Doppler measurements and the gravity wave polarization and dispersion relations. Observed periods and horizontal wavelengths (zonal, meridional components, see text) are shown: 21 days, 1981–82, 414 waves, 80–100 km. (System limits ~ 10–120 minutes, λ_{min} ~ 15 km).

justment is small on a logarithmic plot, and it is an assumption itself.

There is excellent agreement between the new Adelaide λ_h data, the collation, and the Saskatoon data in Fig. 1. A similarly small number of waves lie within or beyond the limiting damping lines (13% and 4%). However, the incorporation of Doppler shifts, appropriate to T^*, would expand the distribution somewhat toward lower and high periods. Such an eventuality is likely to be realistic, as the diurnal tides are strong at Adelaide (e.g., Vincent et al. 1989), and datasets with lengths of 5–6 hours will be affected by significant Doppler shifts depending upon season and local time.

3. Gravity wave data from Urbana

a. Vertical wavelengths

The lidar data from Urbana have also been well discussed in references given in the Introduction. Briefly, "When the vertical wavelength is small ($\lambda_z \leqslant 15$ km), the gravity wave parameters can be measured by observing Na layer profiles and the spatial power spectra of the profiles (Gardner and Shelton 1985)." The spectra provided λ_z, and other amplitude parameters, and "The observed wave periods (T) were usually inferred directly from the layer profiles by measuring the vertical phase velocities. The horizontal wavelengths (λ_h) were then calculated using the dispersion relation," (Gardner and Voelz 1987). It is required (Gardner 1990, private communication), that the, "wave be spatially coherent over an altitude region of approximately 20 km, and over (time intervals) of several tens of minutes." This method clearly *requires* vertical coherence in each case, and as such differs from the radar methods, which place more *emphasis* upon the horizontal coherence. However, as noted in section 2, both radar groups report frequent vertical coherence over several "heights" ($\sim$3–10 km).

Because the vertical wavelength is the directly measured lidar parameter and is also available by means of an internally consistent measurement/calculation from the Saskatoon MF radar using T^*, we choose first to compare those two λ_z sets (Fig. 3), and then follow with a superposition of the derived lidar λ_h upon the collation as in Figs. 1, 2.

In Fig. 3, several sources of λ_z data are shown. First, 71 waves from GRAVNET are shown for 9 days in the winter of 1984, for mesopause heights (70–97 km). The seasonal and height variations are small, and so these are quite similar to data shown by Manson and Meek (1987, 1988) for other altitudes and seasons. These λ_z *must* be plotted against T^* since background winds are known. System limits and eddy diffusion damping limits are shown as before. Second, directly measured λ_z from sources other than the CEDAR Lidar are also plotted. A cross-spectral analysis was applied to neighboring heights, which provided λ_z for *observed* periods (Manson and Meek 1987) during January 1984. A range of wavelengths of inertio-gravity waves (T, 2–6 h) are shown from a variety of sources (Vincent 1984, MF radar; Chanin and Hauchecorne 1981, Lidar, Manson and Meek 1990, MF radar). Rocket data generally have had no periods or uncertain ones, and these are shown as a band of values (e.g., Philbrick et al. 1983). Finally, the new and substantial set of λ_z, T from the CEDAR Lidar are shown as a band: 109 waves from 34 days in summers and winters of 1981–86, for heights from 80–100 km, determined from the Na layer which has maxima near 90 km (Gardner and Voelz 1987). Limits of observation are 2–17 km for λ_z, and $\sim$20 min–12 h for observed period.

Generally there is good overlap of the data from these various sources. The effect of the Doppler shifting upon the Saskatoon GRAVNET λ_z is comparatively small. Significantly, however, all waves with periods greater than 60 minutes have had the calculated λ_z decreased compared to a non-Doppler calculation leading to 10% and 7% of the values being between or beyond the limiting (damping) lines. This is realistic. A few waves with periods T^* less than 10 minutes had increased λ_z values. Otherwise, most λ_z are little affected by the Doppler-shifting, and median values are $\sim$20 km in either case for periods of 20–60 minutes. Other direct measurements of λ_z from radars are similar to the GRAVNET values.

Finally, we turn to the new lidar λ_z data in Fig. 3. Although these overlap with portions of the other sets, their distribution and its line of best fit differ quite dramatically. Most obviously, almost all the values lie between the damping lines (36–300 $m^2 s^{-1}$), although the lidar could resolve waves outside these lines (Gardner 1990, private communication). Doppler shifting would have some effect, especially on waves of smaller horizontal phase velocity and period (Meek et al. 1985, show a comparative figure), but it is unlikely to move many waves into the 20–60 minute and 10–20 km region where the other data reside. This argument is consistent with the distribution of lidar λ_z values in Fig. 3, which is much broader for small λ_z, T. It is also inappropriate to compare lines of best fit for the two main datasets shown here, as the system limits at Saskatoon will dominate that trend. The difference between the lidar and radar datasets is certainly significant, but earlier figures (e.g., Gardner and Voelz 1987) did not show the effect quite as clearly as this. However those authors recognized the problem and noted (p. 4686), "perhaps the Na layer perturbations are dominated by the largest amplitude waves, which are near saturation but influenced primarily by viscous effects, while the lower energy waves . . . are simply not observed." . . . and, "it would appear that the observed waves . . . are more strongly influenced by dissipation effects rather than by saturation." It is important that users and other observers recognize the differences between the radar and lidar data in this figure. There is, however, encouragement in the fact that the directly

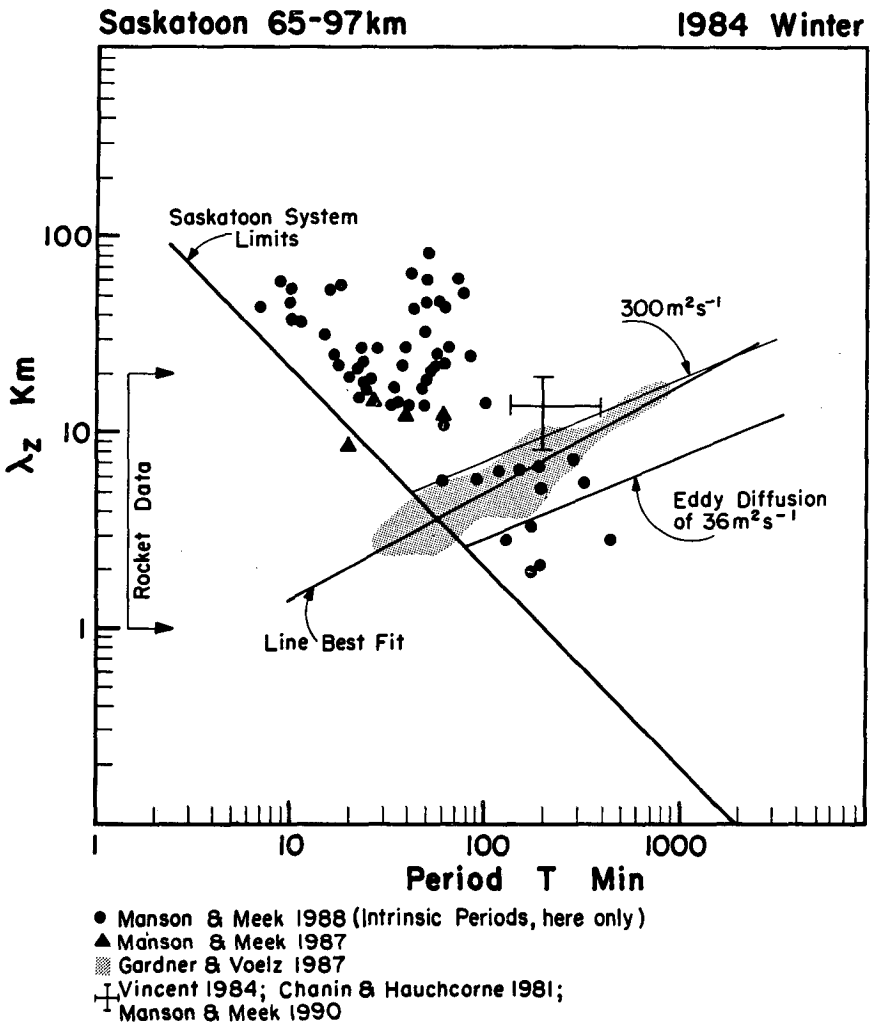

FIG. 3. Vertical wavelengths, λ_z (71) from the Saskatoon GRAVNET system for 9 days in winter 1984, 70–97 km: the dispersion relation and *intrinsic* periods are used to calculate these (Manson and Meek 1988). Direct λ_z measurements using cross spectral analysis, but *observed* periods (Manson and Meek 1987) are added for January 1984. Wavelengths of inertio-gravity waves (2–6 hours observed) are shown by two bars (Vincent 1984; Chanin and Hauchcorne 1981; Manson and Meek 1990). Rocket data generally have no (or uncertain) periods (e.g., Philbrick et al. 1983). Finally, *observed* λ_z (109) from 34 days in summer and winter 1981–86 from lidar observations (*observed* period) are shown with toning (Gardner and Voelz 1987).

measured lidar λ_z of small value agree with the smallest λ_z from the less direct radar technique, suggesting that the two techniques are complementary.

It should also be noted that the Urbana group has operated the lidar in the Rayleigh scattering mode to obtain gravity wave data in the stratosphere (Gardner et al. 1989). These are not discussed in any detail here for two reasons: one, we are comparing mesospheric data and differences in distribution of λ_z, λ_h may be expected in the stratosphere; and two, there is extensive comparison within that paper of stratosphere–mesosphere gravity waves. It is worthwhile observing that their other λ_z, T plot also has a line of best fit with a positive slope, but it is even greater, passing through the 1-km point at ~50 minutes and through similar values to Fig. 3 at 500 minutes. The scatter at λ_z is somewhat greater, but overall the form of the distribution is quite different from the mesospheric radar data.

b. Horizontal wavelengths

The final Fig. 4. compares derived λ_h from the Na lidar data with the collation of Reid (1986). The lidar values lie almost completely (87%) between the damping lines for eddy viscosity of 36 and 300 $m^2 s^{-1}$, with an even narrower distribution than in Fig. 3. This last observation is nicely explained by Gardner and Voelz

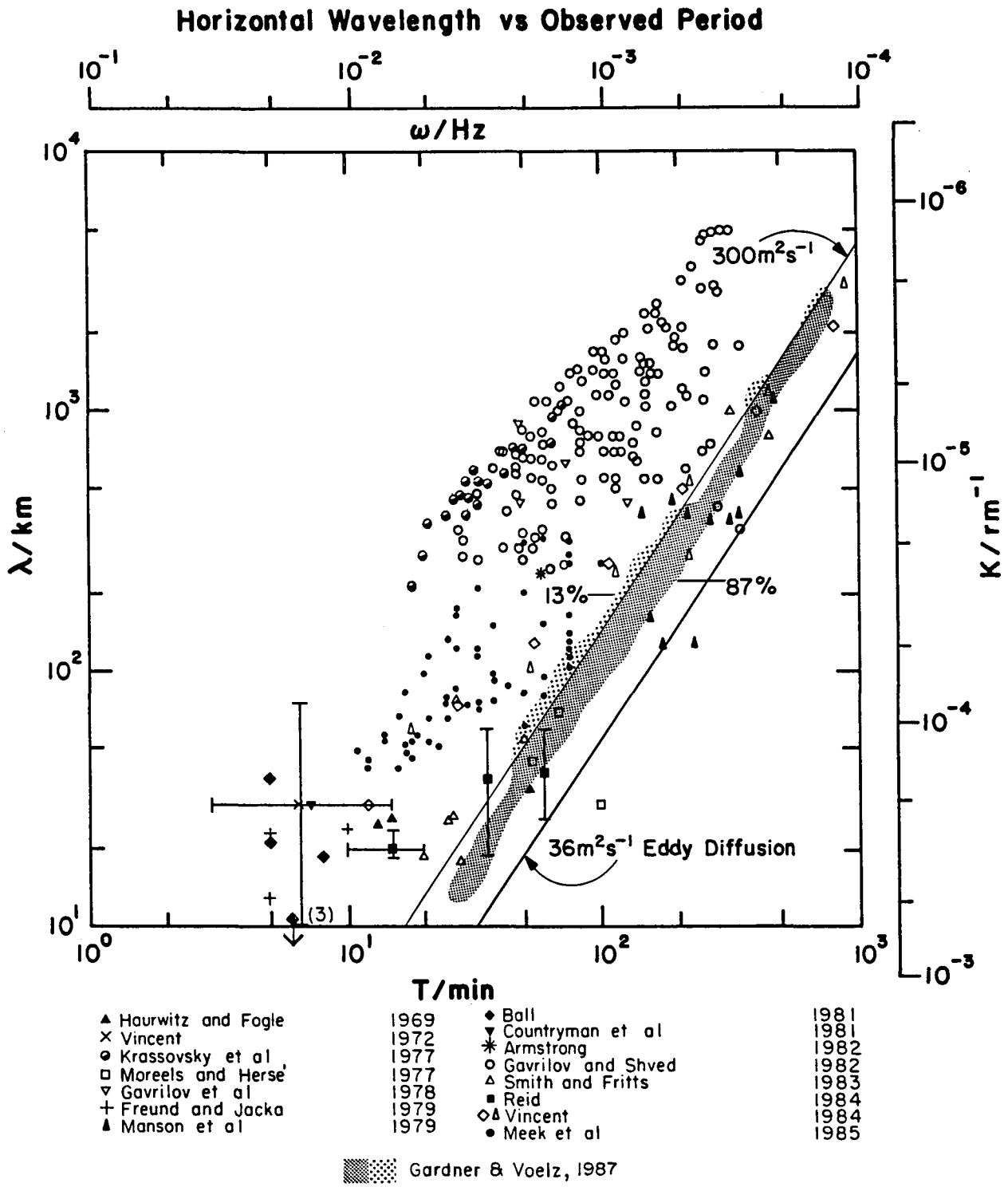

FIG. 4. As in Fig. 1, but the additional data are now from Gardner and Voelz (1987). Lidar sounding (sodium layer) provides vertical wavelengths at observed periods, and use of the dispersion equation provides the plotted horizontal wavelengths: 34 days, 1981–86, 109 waves in summer and winter 80–100 km. (System limits: ~20 minutes–12 hours, λ_z 2–17 km).

(1987), who conclude that, "plotting λ_h versus T (observed) tends to compensate for the measurement errors in vertical phase velocity and λ_z." The differences between Figs. 1, 2, and 4 are certainly very obvious, but expected after the discussion of λ_z values in Fig. 3.

It is remarkable that the lidar values of λ_z, λ_h are so narrow in their distribution and also so close to the limits for waves undergoing damping due to eddy viscosity. The comments by Gardner and Voelz (1987) above are certainly appropriate. However, one would have expected such an effect, if it were to occur, for a plot of wavelength versus intrinsic period T^*, rather than the observed period. We reiterate, without wishing to belabor the point, that the transition of lidar data from Fig. 3 to 4 is formally incorrect, although frequently used for gravity-wave investigators (including this author) to obtain a likely range of values for the "other" wavelength.

In fact, it is quite possible that Doppler effects were not very important for these observing conditions. The mean winds at lower midlatitudes are rather weak near 95 km in the solstices (<20 m s^{-1}, Manson et al. 1987), and tidal amplitudes at nearby Durham, (43°) are smaller than at Adelaide (there the 24-hour is large, Vincent et al. 1989), or Saskatoon (there the 12-hour is larger, Manson et al. 1989). Also, many of the observations with the lidar were for longer periods (>100 minutes) than with the radars, where the observed periods were $\leqslant 120$ minutes. At these longer periods the horizontal phase velocities are typically greater, minimizing Doppler-shifting, and the effect of background oscillating winds associated with the tides will tend to be averaged out. We note that the stratospheric λ_h values (Gardner et al. 1989) have a slope and distribution very similar to Fig. 4, but displaced downward by a factor of two or so.

4. Conclusion

There is excellent agreement between the earlier (Reid 1986) collation of gravity wave horizontal wavelengths, obtained from optical and radar systems, and the new significant datasets from the MF radars at Adelaide and Saskatoon. In general, a small percentage (12%–17%) of the values lie between or beyond lines appropriate to significant viscous damping of these waves, i.e., eddy diffusion values of 36–300 m^2 s^{-1}.

In contrast, the majority of values ($\sim$90%) of vertical wavelength λ_z measured by the lidar (sodium) system at Urbana lie between these viscous damping limits, whereas only 17% of vertical wavelengths obtained from the Saskatoon radar, using the dispersion relation with the appropriate intrinsic periods, lie as close to the damping lines. Estimates of horizontal wavelength λ_h from the lidar λ_z data, using the dispersion relation with *observed* periods, also lie close to, and mainly between (87%), these limits. It is argued that the Doppler shifting effects at Urbana were probably small; and that, in agreement with the Urbana investigators, the, "sodium layer perturbations are dominated by the largest amplitude waves, which are near saturation but influenced primarily by viscous effects . . ."

Given the differences between the distributions of gravity wave characteristics due to various types of system–data limits and physical selectivity, it is vital that potential users consider these before use, and that observers clearly state or mark those limits. The radar and lidar systems appear to be complementary in that context, and joint campaigns (R. A. Vincent, C. S. Gardner) will undoubtedly be profitable.

Acknowledgments. The financial support of the Natural Sciences and Engineering Research Council and the Atmospheric Environment Service, both of Canada, is gratefully acknowledged, also of the Institute of Space and Atmospheric Studies, through the University of Saskatchewan, Saskatoon. The author thanks Iain Reid for providing the background figure for this paper. The assistance of Edison del Canto in drafting, and Pat Wilson in preparing the manuscript, are also gratefully acknowledged.

REFERENCES

Chanin, M. L., and A. Hauchecorne, 1981: Lidar observations of gravity and tidal waves in the stratosphere and mesosphere. *J. Geophys. Res.*, **86,** 9715–9721.

Fritts, D. C., 1984: Gravity wave saturation in the middle atmosphere: a review of theory and observations. *Rev. Geophys.*, **22,** 275–308.

——, and P. K. Rastogi, 1985: Convective and dynamical instabilities due to gravity wave motions in the lower and middle atmosphere: theory and observations. *Radio Sci.*, **20,** 1247–1277.

Gardner, C. S., and J. D. Shelton, 1985: Density response of neutral atmosphere layers to gravity wave perturbations. *J. Geophys. Res.*, **90,** 1745–1754.

——, and D. G. Voelz, 1987: Lidar studies of the nighttime sodium layer over Urbana, Illinois. Part 2: Gravity wave. *J. Geophys. Res.*, **92,** 4673–4694.

——, M. S. Miller, and C. H. Liu, 1989: Rayleigh lidar observations of gravity wave activity in the upper stratosphere at Urbana, Illinois. *J. Atmos. Sci.*, **476,** 1838–1854.

Gossard, E. E., and W. H. Hooke, 1975: *Waves in the Atmosphere.* Elsevier Scientific, 456 pp.

Hines, C. O., 1974: *The Upper Atmosphere in Motion.* AGU, 1027 pp.

Hocking, W. K., 1985: Turbulence in the region 80–120 km. *Middle Atmosphere Program Handbook,* Interim CIRA, 290–304.

Manson, A. H., and C. E. Meek, 1987: Small-scale features in the middle atmosphere wind field at Saskatoon, Canada (52°N, 107°W): an analysis of MF radar data with rocket comparisons. *J. Atmos. Sci.*, **44,** 3661–3672.

——, and ——, 1988: Gravity wave propagation characteristics (60–120 km) as determined by the Saskatoon MF radar (Gravnet) system: 1983–85 at 52°N, 107°W. *J. Atmos. Sci.*, **45,** 932–946.

——, and ——, 1990: Inertio-gravity waves and nonlinear tidal effects in the upper middle atmosphere at Saskatoon (52°N). *Planet. Space Sci.*, in press.

——, ——, M. Massebeuf, J. L. Fellous, W. G. Elford, R. A. Vincent,

R. L. Craig, R. G. Roper, S. Avery, B. B. Balsley, G. J. Fraser, M. J. Smith, R. R. Clark, S. Kato and T. Tsuda, 1987: Mean winds of the upper middle atmosphere (~70–110 km) from the global radar network: comparisons with CIRA 72 and new rocket and satellite data. *Adv. Space. Res.*, **7**, 143–153.

——, ——, H. Teitelbaum, F. Vial, R. Schminder, D. Kurschner, M. J. Smith, G. J. Fraser and R. R. Clark, 1989: Climatologies of semidiurnal and diurnal tides in the middle atmosphere (70–110 km) at middle latitudes (40–55°). *J. Atmos. Terr. Phys.*, **51**, 579–594.

Meek, C. E., I. M. Reid, and A. H. Manson, 1985: Observations of mesospheric wind velocities, I. Gravity wave horizontal scales and phase velocities determined by spaced wind observations. *Radio Sci.*, **20**, 1363–1382.

Philbrick, C. R., K. U. Grossman, R. Hennig, G. Lange, D. Krankowsky, D. Offerman, F. J. Schmidlin and U. von Zahn, 1983: Vertical density and temperature structure over Northern Europe. *Adv. Space Res.*, **2**, 121–124.

Reid, I. M., 1984: Radar studies of atmospheric gravity waves. Ph.D. thesis, University of Adelaide, Australia,

——, 1986: Gravity wave motions in the upper middle atmosphere (60–110 km). *J. Atmos. Terr. Phys.*, **48**, 1057–1072.

——, 1989: Observations of gravity wave scales, fluxes, and saturation during MAP. *Hand. Middle Atmos. Prog.*, **27**, 87–103. [SCOSTEP Secretariat, University of Illinois, Urbana, 61801.]

——, and R. A. Vincent, 1987: Measurements of the horizontal scales and phase velocities of short period mesospheric gravity waves at Adelaide, Australia. *J. Atmos. Terr. Phys.*, **49**, 1033–1048.

Vincent, R. A., 1984: Gravity-wave motions in the mesosphere. *J. Atmos. Terr. Phys.*, **46**, 119–128.

——, and I. M. Reed, 1983: HF Doppler measurements of mesospheric gravity wave momentum fluxes. *J. Atmos. Sci.*, **40**, 1321–1333.

——, T. Tsuda, and S. Kato, 1989: Asymmetries in mesospheric tidal structure. *J. Atmos. Terr. Phys.*, **51**, 609–616.